The Climate Change Impact on Power Grid Transmission Capacity

Sergio Daniel Montana Salas, Andrea Michiorri

The Climate Change Impact on Power Grid Transmission Capacity

Montana Sergio-Daniel, Andrea Michiorri

February 2024

Abstract

Proposing practical solutions to mitigate climate change effects on the electrical power system requires a comprehensive understanding and quantification. By conducting an assessment at high grid resolution, this article explores the impact of climate on transmission network capacity, employing established thermal models and a regional expansion plan. The results indicate average reductions of 1.53%, 2.3%, and 0.2% for overhead lines, power transformers, and underground cables, respectively. We propose a quasi-Dynamic Thermal Rating method to counter these effects, estimating maximum capacity. This approach enhances component capacity by an average of up to 35% during winter at the power transformers and up to 14% during nighttime hours for overhead lines. This solution constitutes a viable alternative for electricity operators, to address the dilemma between the necessity of reducing the failure rate/decrease in capacity, and the imperative need for new investments in transmission assets.

Keywords: Climate change, Dynamic Thermal Rating , Power Systems

1 Introduction

Climate change projections estimate an average atmospheric temperature increase of 2-4^{o}C until the end of the century[1, 2]. This will directly and negatively impacts the electric power system, affecting transmission capacity, generation, demand, and congestion.

Regarding transmission, which is the main focus of this study, the current carrying capacity of Overhead Lines (OHL), Power Transformers (PT), and Underground Cables (UGC) is determined, among other factors, by their ability to dissipate joule losses into the external environment. In turn, this depends on ambient temperature: the lower the external temperature, the higher the transmission capacity, and vice versa. For instance, in the United States, the impact of global warming is anticipated to cause a reduction in OHL capacity within the range of 1.9% to 5.8% [3].

In reference to power generation, higher temperatures leads to a reduction in production capacity: on the one hand, a higher ambient temperature increases the sink temperature in thermodynamic cycles, reducing overall conversion efficiency. On the other hand, it reduces air density, in turn reducing, the mass flow intake of fossil fuel generators. Furthermore, factors such as water discharge temperatures and diminishing water flows are anticipated to impact over 80% of the world's thermal power plants due to drought and shifting seasonal patterns, as detailed in [4].

Regarding power demand, this tends to grow with higher ambient temperature due to load thermosensitivity driven by air conditioning. This is in turn accentuated by the growing penetration of air cooling in power systems, including in developing countries. In [5], the expected annual demand variation in different scenarios ranges from -2.7% to 5.7% on average and is further exacerbated during heat waves, culminating in an increase of up to 21%[6].

The combination of lower transmission capacities, lower generation, and higher load can increase the likelihood of congestion in the transmission and distribution infrastructure. This leads to inefficiency and spikes in local power prices, exacerbating current trends which, for example, resulted in a cost of roughly $4.8 billion in 2016, as reported by the U.S. Department of Energy (DOE) in 2018 [7].

Among the solutions proposed to alleviate network congestion problems, Dynamic Thermal Rating (DTR) [8, 9, 10, 11] is actively being deployed on critical lines. This is a technology aiming at identifying the real-time current carrying capacity of network components, which is, in general, higher than its Static Thermal Rating (STR). On the one hand, this value is strongly weather-dependent; on the other, DTR allows the removal of network congestions and associated curtailments and delays, and can remove network reinforcements whilst improving reliability.

Various studies have incorporated DTR into power system expansion plans[12, 13] and highlighted its importance in RES integration and penetration [14, 15, 16, 17, 18].These studies employ control and sensing devices [19, 20] or data-driven probabilistic methods to calculate the rating of OHL [21]. All these studies yield generalized findings on the efficacy of DTR, among which the following can be emphasized: a) Decreased system congestion costs due to less generator re-dispatching. b) Reduction or postponement of investments required for reinforcing or expanding existing assets. c) Grid operational flexibility to enhance facilitated integration of RES.

In this study, we leverage historical and projected meteorological variables at different geographical points on the power system component's location. Through this data, we calculate the maximum current that the system can carry at any point in time without any section's temperature surpassing the predefined maximum threshold, employing DTR methodology. By doing so, we emphasize the significant potential of DTR in enhancing power system flexibility. To reinforce this assertion, we analyze power system planning within the Generation and Transmission Expansion Plan (G&TEP) framework using a tool for modeling hybrid power systems.

This is made possible by the availability of widely accepted component thermal models [22, 23, 24], open energy data models [25] and quantitative climatic projections such as the Representative Concentration Pathways (RCP) [26] and Shared Socio-economic Pathways (SSPs) [27], which constitute a valuable toolset for assessing regional climate changes and their specific impacts on the energy sector.

As a main contribution, this research aims to quantify the impact of climate change on power system transmission capacity. It also proposes quasi-Dynamic Thermal Rating (qDTR) as the primary solution to recover lost transmission capacity, facilitating the connection of renewable resources and reducing network costs.

2 Result and Discussion

This study applies qDTR to estimate the maximum allowable currents of power transmission components using historical ($qDTR_H$, from 1970 to 2022) and future weather projections for Europe ($qDTR_{RCPx}$, where x represents the RCP scenario evaluated from 2023 to 2070).

Firstly, the use of $qDTR_H$ instead of STR_H increases average transmission capacity in the region of 14.2%, 17.4% and 3.7% for OHL, PT and UGC respectively (see Table 1, first row). The results indicate an average reduction in the transmission capacity of the network, ranging from 1.3% to 8.6% as shown in Figure 1. This outcome is a consequence of an increase in ambient temperature of between 1.3% to 2.4%.

We then quantify the climate impact of transmission network capacity for three main components: PT, OHL, and UGC. The results are shown in Table 1. Demonstrate how average component ratings can drop from 0.4% to 1.53% (OHL), creating additional costs for the network in the region of 0.006% to 0.064%. Figure 4 reports the average OHL rating variation expected in Europe in the RCP 2.6 Scenario.

Figure 1 visually illustrates the trend, presenting the rating evolution over the next five decades for the European network's OHL [28] under low, medium, and high emission scenarios. These ratings are then incorporated into a G&TEP, enabling the calculation of optimal investments and operating costs. Across the three scenarios, not considering climate evolution would result in costs underestimations in the region of 0.1% to 0.2% for CAPEX, -6.2% to 3.1% for OPEX and 9.3% to 70.2% for renewable curtailment.

The next three sections show firstly the increased transmission capacity allowed by qDTR, then the impact of climate change on network transmission capacity calculated by qDTR and finally the effect of climate change on network planning.

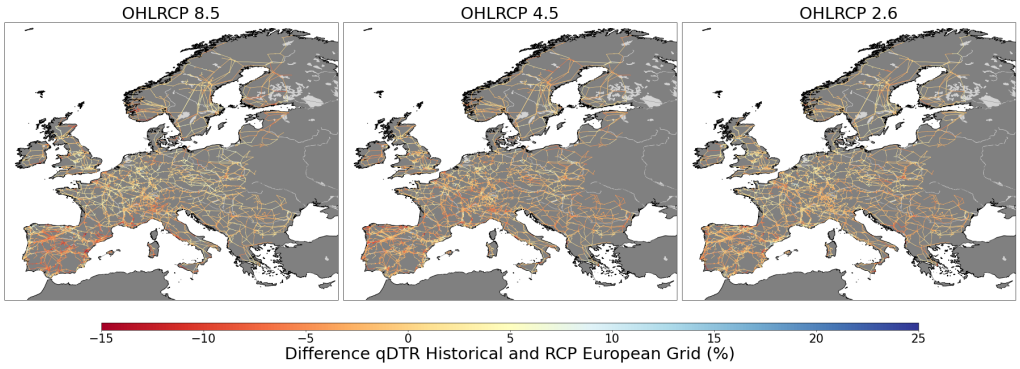

Figure 1: Climate impacts on transmission capacity, difference in capacity for qDTR in the month of June under the average RCP 2,6, 4.5 and 8.5 scenario for OHL.

2.1 Benefits of qDTR vs STR

We start by analyzing the benefit of using qDTR instead of STR in network operations. Figure 2 reports the percentage variation in average transmission capacity for OHL, PT, and UGC, respectively, in Europe. In this case, $qDTR_H$ and STR_H are calculated using historical values from 1970 to 2020. Note that $qDTR_H$ are always above STR_H in all studied regions.

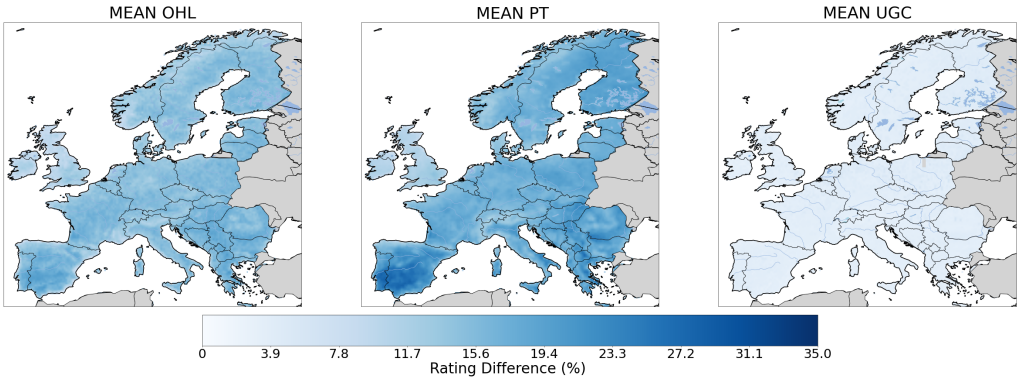

Figure 2: Geographical distribution of the mean Historical $\Delta_{\%}(\mathrm{qDTR_H}, \mathrm{STR_H})$ difference at the country level. This is performed for the three main power components (OHL, PT and UGC).

Fig. 3 shows the yearly and hourly variations of $\mathrm{qDTR_H}$ for the three components in southeast France. For OHL and PT, we can see that in daily summer hours, $\mathrm{qDTR_H}$ are lower than $\mathrm{STR_H}$. On the contrary, in winter and night hours, $\mathrm{qDTR_H}$ are far higher, resulting in a larger overall transmission capacity. Concerning UGC, as expected, their qDTR do not change during the day, due to the high thermal inertia of the soil. Another aspect worth mentioning is the daily and yearly variations of $\mathrm{qDTR_H}$. For the three components considered, the yearly qDTR variation range in the region is ±15% from the highest to the lowest value, driven by temperature variations.

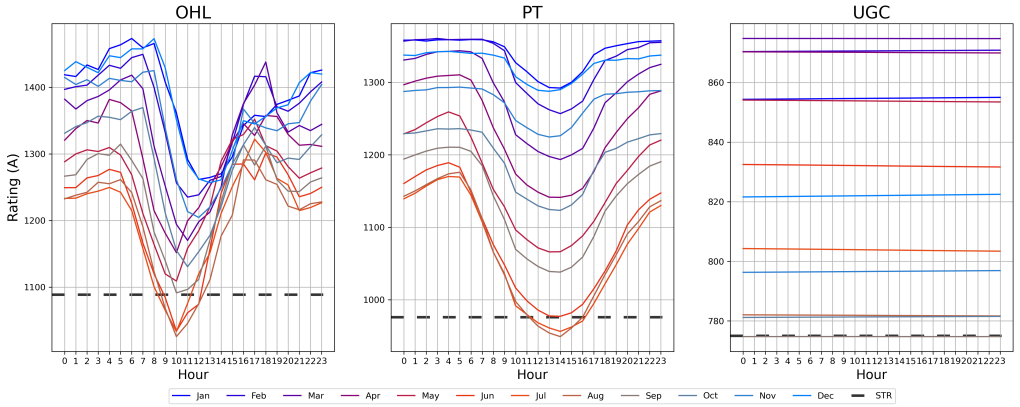

Figure 3: $\mathrm{qDTR_H}$ calculated for each month/hour combination for OHL, PT and UGC calculated in the node of Tavel (southeast France). Colors represent months from the coldest (blue) to the warmest (red). Yearly static ratings are represented by a dashed black line.

2.2 Impact of climate change on network transmission capacity

When qDTR are calculated using projections for the next decades instead of weather data relative to past years, the effect of a temperature rise predicted by climatic projections becomes apparent.

Table 1 reports the average and extreme values for the difference in transmission capacity calculated using data on historical weather and expected future weather. In all three scenarios, transmission capacity is expected to drop. Transformers are the component with the highest variation (from -1.0% to -2.3%) followed by OHL (from - 0.4% to -1.53%) and UGC (from -0.1% to -0.2%). This is explained by the fact that the OHL rating is mainly influenced by air temperature and wind speed, whilst the PT rating is only influenced by air temperature. Often hottest hours are also characterized by not null wind speeds, reducing the derating effect of temperature. For UGC, the much narrower temperature variation of the soil prevents large rating drops. The worst cases simulated show a maximum reduction of -3.9%, -5.1% and -1% for the ratings of OHL, PT and UGC, respectively.

Figure 4 shows the spatial distribution of the rating variations summarized in 1. The spatial variation of average transmission capacity for the three components is reported above.

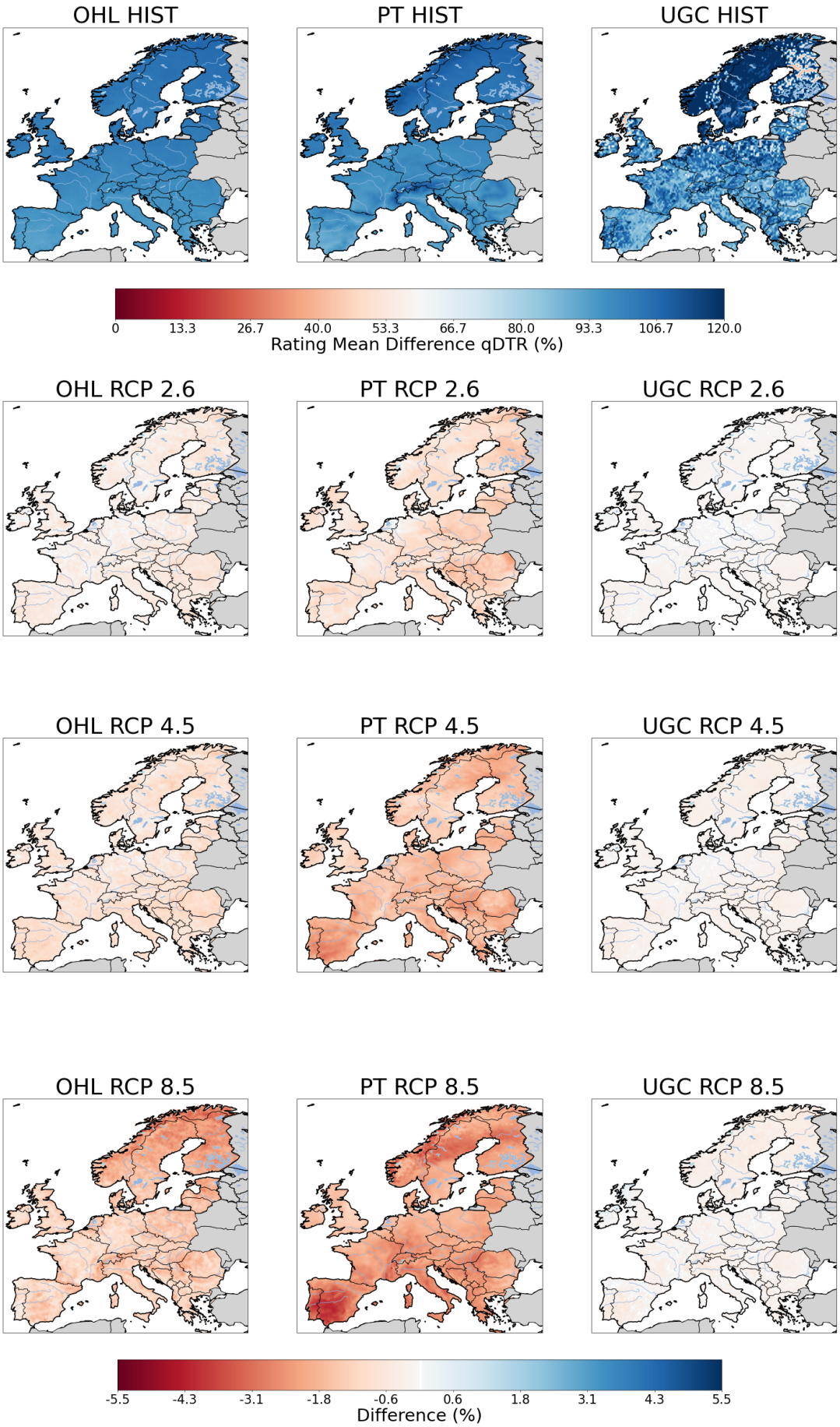

Figure 4: Geographical distribution of the mean qDTR difference at the country level over fifty years for the RCPs and the historical reanalysis. This is performed for the three main power components (OHL - PT and UGC). The first row reflects the difference in the variation of the historical average for the region, and the subsequent rows illustrate the variation in the average for each of the RCPs.

Table 1: Variation for the three scenarios with respect to historical values for qDTR for the European region.

Description	Component		
	OHL	PT	UGC
$\Delta_{\%}(\mathbf{qDTR_H, STR_H})$[1]			
Mean	14.2	17.4	3.74
$\Delta_{\%}(\mathbf{qDTR_H})$			
Max	10.7	17.4	29.6
Min	-9.4	-16.4	-57.8
$\Delta_{\%}(\mathbf{qDTR_{RCP2.6}, qDTR_H})$[3]			
Mean	-0.4	-1.0	-0.1
Max	-1.4	-2.4	-0.5
Min	0.75	0.3	0.8
$\Delta_{\%}(\mathbf{qDTR_{RCP4.5}, qDTR_H})$[3]			
Mean	-0.7	-1.7	-0.2
Max	-1.7	-3.2	-0.6
Min	0.9	-0.6	0.5
$\Delta_{\%}(\mathbf{qDTR_{RCP8.5}, qDTR_H})$[3]			
Mean	-1.53	-2.3	-0.2
Max	-3.9	-5.1	-1
Min	0.32	-0.8	1.0

The first row shows the spatial variability of $qDTR_H$ in Europe, which is in the region of 20%, 30% and 90% for OHL, PT and UGC. The lower variability of OHL is given, as explained above, by the double dependency from wind and air temperature of its rating. The very high variability of UGC ratings on the contrary is given by the variety of soils in the different regions, which considerably impacts thermal diffusivity and moisture retention. The following three rows show the percentage variation in qDTR in Europe according to the different climate scenarios considered. The variations are almost unanimously negative, with peaks in central Spain, the Arctic and mountainous regions. As mentioned above, UGC presents lower variations because of the high soil inertia.

Finally, the heat map in Fig. 5 represents the temporal variation by month and hour of $qDTR_{RCP}$ on a specific node of the network. The effect of increased ambient temperature in the three RCP scenarios is shown in Fig. 5. The observed variations, which are moderately significant, for instance translate into an average rating reduction of -2.3% in July for $qDTR_{RCP\ 8.5}$ and -0.7% for $qDTR_{RCP\ 4.5}$ in the PT. This could be translated in terms of variation in the risk level regarding the equipment's lifetime for the network operator. On the other hand, the opposite effect can also be observed in specific months and hours, such as -0.9% on February mornings for $qDTR_{RCP\ 8.5}$, +0.7% for $qDTR_{RCP\ 4.5}$ and +0.02 $qDTR_{RCP\ 2.6}$.

2.3 Impact of climate change on network costs

This section examines investment decisions within the Generation and Transmission Expansion Plan, incorporating climate-variant supply and qDTR for power system components.

To achieve this, we use a network model from the PyPSA [25] package, applying STR_H and $qDTR_{RCP}$ calculated with historical or climate projections using weather data. The network model is then used to carry out a G&TEP in order to estimate changes in CAPEX, OPEX, and renewable curtailment

The results are summarized in Table 2, which shows:[1] the results of a baseline simulation with STR,[2] the improvements obtained using $qDTR_H$ instead of STR_H, and [3] the error incurred when using historical weather instead of climate projections in $qDTR_{RCP}$ calculations. In each case, the CAPEX and OPEX are reported for different assets, such as fossil fuel generators, renewable generators, nuclear generators, transmission lines, and storage. For renewable generators, the amount of expected curtailment is also reported.

When comparing the minimum and maximum emission scenarios in Europe under the same projection, a difference of 154 MWh is observed in the dispatch energy for onshore wind. Conversely, in France, electricity generation CO_2 targets remain relatively stable for nuclear, run of river, solar, coal lignite,

[1]The average additional transmission capacity provided by qDTR in place of STR, calculated from historical data.
[2]The spatial variation on the continent of qDTR, calculated from historical data.
[3]The variation of transmission capacity calculated with the specific climatic scenario versus historical weather

Table 2: Variation (in %) for the three scenarios with respect to yearly fix rating and costs, the scenarios covering historical static (STR_H)[1], historical ($qDTR_H$)[2] and projected ($qDTR_{RCP}$)[3]

Description			**STR_H** [1]			**$\Delta(qDTR_H, STR_H)$** [2]			**$\Delta(qDTR_{RCP}, qDTR_H)$** [3]		
Region	**RCP**	**Technology**	**CAPEX**(BEur)	**OPEX**(BEur)	**Curtailment**(GWh)	**CAPEX**	**OPEX**	**Curt.**	**CAPEX**	**OPEX**	**Curt.**
EUROPE	2.6	Fossil	60.8E+0	6.3E+0	0.0E+0	-1.5E-04	-2.1E-03	-	2.1E-05	2.3E-04	-
		Renewable	58.8E+0	2.4E+0	2.3E+0	-8.8E-04	4.6E-03	-1.7E-01	2.5E-04	-7.6E-04	9.3E-02
		Nuclear	88.8E+0	9.5E+0	0.0E+0	-3.4E-05	6.2E-04	-	2.5E-06	-8.3E-05	-
		Lines	5.6E+0	1.0E+0	0.0E+0	-5.6E-04	2.0E-02	-	2.5E-04	1.7E-03	-
		Storage	27.6E+0	3.8E-3	0.0E+0	0.0E+00	-1.9E-04	-	0.0E+00	9.0E-05	-
		Total	241.5E+0	19.3E+0	2.3E+0	-2.8E-04	1.2E-03	-1.7E-01	7.2E-05	2.5E-05	9.3E-02
	4.5	Fossil	60.8E+0	6.3E+0	0.0E+0	-3.2E-05	-1.6E-03	-	1.3E-04	-1.2E-04	-
		Renewable	58.7E+0	2.4E+0	1.9E+0	-2.5E-04	2.5E-03	-5.9E-02	7.5E-04	-3.0E-03	1.7E-01
		Nuclear	88.8E+0	9.6E+0	0.0E+0	-2.8E-05	2.4E-04	-	4.7E-05	-3.9E-04	-
		Lines	5.6E+0	1.02E+0	0.0E+0	-3.4E-05	-3.1E-02	-	5.6E-04	-3.7E-02	-
		Storage	27.6E+0	3.9E-3	0.0E+0	0.0E+00	3.9E-02	-	0.0E+00	-2.7E-02	-
		Total	241.4E+0	19.3E+0	1.9E+0	-8.1E-05	-1.8E-03	-5.9E-02	2.5E-04	-2.6E-03	1.7E-01
	8.5	Fossil	60.8E+0	6.3E+0	0.0E+0	-1.3E-04	-1.8E-03	-	3.4E-04	0.0E+00	-
		Renewable	58.8E+0	2.4E+0	2.3E+0	-9.6E-04	4.9E-03	-1.8E-01	2.4E-03	-8.2E-03	7.0E-01
		Nuclear	88.8E+0	9.5E+0	0.0E+0	-5.7E-05	6.1E-04	-	1.6E-04	-9.6E-04	-
		Lines	5.6E+0	1.0E+0	0.0E+0	-5.4E-04	1.0E-01	-	1.9E-03	-7.8E-02	-
		Storage	27.6E+0	3.8E-3	0.0E+0	0.0E+00	2.2E-02	-	0.0E+00	3.9E-02	-
		Total	241.5E+0	19.3E+0	2.3E+0	-3.0E-04	3.3E-04	-1.8E-01	7.7E-04	-1.1E-03	7.0E-01
FRANCE	2.6	Fossil	1.9E+0	2.2E-4	0.0E+0	4.3E-04	-5.3E-04	-	-7.6E-05	-8.1E-05	-
		Renewable	5.1E+0	1.9E-2	2.4E-1	-1.2E-03	-4.3E-02	-6.0E-01	5.1E-05	-1.4E-03	2.6E-02
		Nuclear	4.4E+1	3.4E+0	0.0E+0	-1.7E-05	1.0E-05	-	5.2E-06	-1.9E-07	-
		Lines	2.0E+0	1.5E-1	0.0E+0	-1.4E-04	-1.0E-01	-	1.1E-05	7.5E-02	-
		Storage	2.3E+0	3.4E-4	0.0E+0	0.0E+00	1.1E-02	-	0.0E+00	1.5E-05	-
		Total	55.8E+0	3.6E+0	236.8E-3	-1.1E-04	-6.7E-03	-6.0E-01	6.5E-06	4.3E-03	2.6E-02
	4.5	Fossil	1.9E+0	2.2E-1	0.0E+0	5.2E-05	-1.1E-03	-	8.7E-05	4.7E-04	-
		Renewable	5.1E+0	1.9E-2	1.9E-1	-2.4E-04	-3.0E-02	-2.8E-01	-1.0E-04	7.2E-03	-4.1E-02
		Nuclear	4.4E+1	3.4E+0	0.0E+0	-2.7E-05	-5.7E-05	-	-2.0E-06	-4.4E-06	-
		Lines	2.0E+0	1.5E-1	0.0E+0	-3.3E-05	1.5E-01	-	4.9E-06	-9.9E-02	-
		Storage	2.3E+0	3.4E-4	0.0E+0	0.0E+00	-1.2E-02	-	0.0E+00	1.2E-02	-
		Total	55.8E+0	3.8E+0	189.0E-3	-4.2E-05	8.7E-03	-2.8E-01	-7.6E-06	-6.7E-03	-4.1E-02
	8.5	Fossil	1.9E+0	2.2E-1	0.0E+0	-1.6E-05	3.3E-04	-	1.6E-05	3.6E-04	-
		Renewable	5.1E+0	1.9E-2	1.5E-1	-1.9E-04	-6.4E-03	-1.3E-01	2.4E-04	7.5E-03	3.7E-01
		Nuclear	4.4E+1	3.4E+0	0.0E+0	2.4E-06	7.9E-05	-	5.0E-06	4.4E-05	-
		Lines	2.0E+0	1.5E-1	0.0E+0	-3.1E-05	1.3E-01	-	1.1E-04	-4.8E-02	-
		Storage	2.3E+0	3.4E-4	0.0E+0	0.0E+00	-1.2E-02	-	0.0E+00	4.2E-04	-
		Total	55.8E+0	3.8E+0	153.2E-3	-1.7E-05	8.1E-03	-1.3E-01	3.0E-05	-3.2E-03	3.7E-01

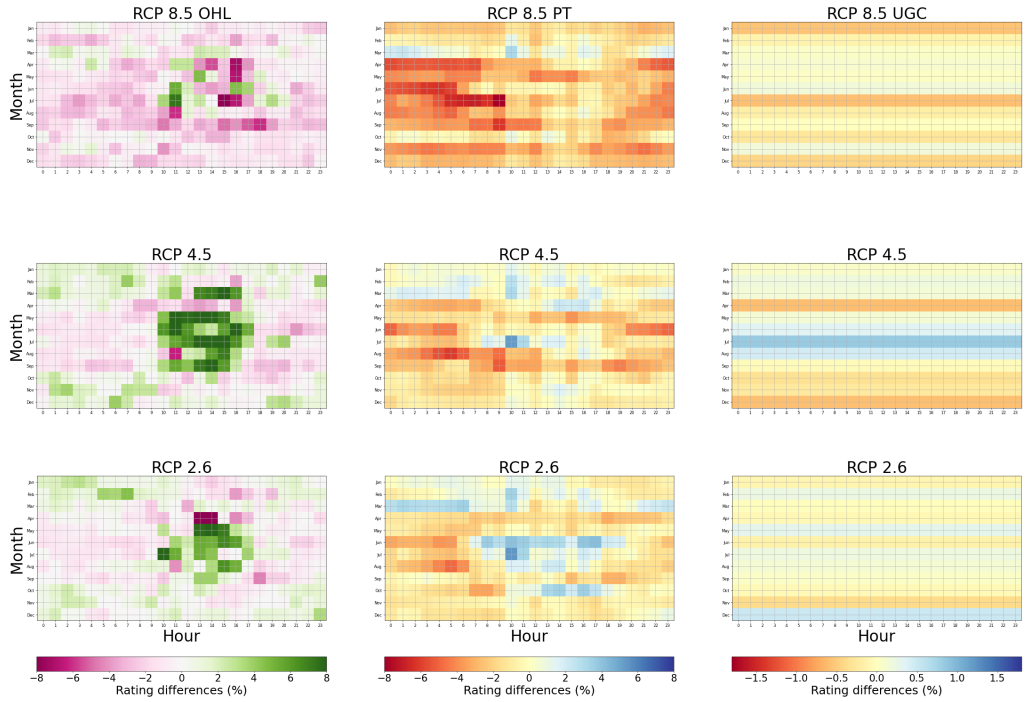

Figure 5: Difference in the calculated qDTR month/hour between historical values and RCP projections 2.6, 4.5, 8.5. This is performed for the three main power components (OHL - PT and UGC), in a node located in Tavel, southeast France.

nuclear, and oil, indicating their consistent performance in the context of the analyzed DTR scenarios (from -0.25% to 0.32%).

The impact of climate change is linked to qDTR in Transmission Expansion Plans (TEPs). In scenarios marked by increased greenhouse gas emissions, the transmission capacity requirements are subject to a substantial increase of 49% in Europe and 98% in France for the 2050 scenario, as evidenced in the high-emission scenario RCP 8.5. However, It must be noted that using qDTR instead of static rating reduces curtailment by up to 60% in renewables in the French case for the 2.6 scenario due to the massive expansion of renewables, and 17% in the European case.

Concomitantly, as emissions continue to escalate, resulting in elevated temperatures across Europe, the vulnerability to energy curtailments becomes more pronounced. In specific scenarios like RCP 8.5, characterized by high emissions, the likelihood of curtailments increases from 9.3% to 70% in Europe and from 2.6% to 36.6% in France. In the field of renewable technology, onshore wind curtailment displays notable variability across CO_2 budgets ranging from up to 1.25 GW for Europe in the low-emission scenario employing STR_H, to 1.02 GW in the high-emission scenario using $qDTR_H$. Other technologies, such as solar PV, also manifest changes, albeit with less magnitude, across CO_2 budget scenarios $qDTR_{RCP\ 2.6}$ and $qDTR_{RCP\ 8.5}$, indicating a shift from 233.64 to 129.52 MW.

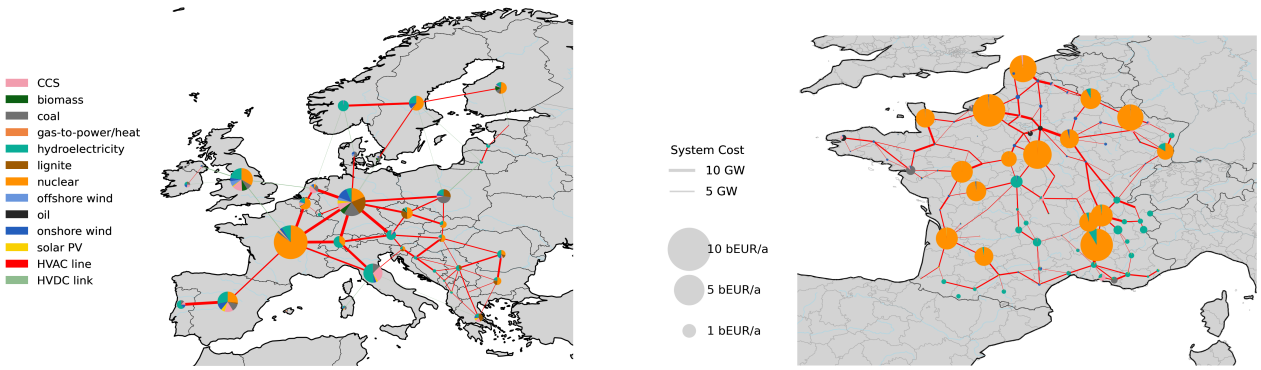

(a) European electricity system infrastructure

(b) French electricity system infrastructure

Figure 6: Regional G&TEP evaluated with Static Annual Rating at 0.1% probability of overload

2.4 Discussion

By conducting an assessment at high grid resolution, this analysis takes a close look at the climate impact on transmission network capacity by utilizing established thermal models and a regional expansion plan for generation and transmission by 2050. Using the qDTR method to estimate maximum capacity with a low-risk exceedance probability, our findings reveal substantial reductions in the mid-term high-emission horizon for power transformers and overhead lines. In contrast, for underground cables, the reductions are more modest, highlighting their lower sensitivity to potential climate changes; this demonstrates that the heat balance has a memory, i.e., soil moisture anomalies may persist for weeks or even months (monthly rate change less than 5%.).

Mitigating the risk of exceeding the Static Season Rating, attributed to the likelihood of overload in unfavorable meteorological conditions that impede heat dissipation (e.g., low wind speed, high temperature, low precipitation), is achieved with a reduction of up to 99.998%. This improvement positively contributes to the reliability of the transmission system. However, as part of a trade-off, qDTR allow us to optimize energy utilization during the colder nighttime hours in both summer and winter. This is particularly crucial for managing nighttime winter load peaks. The observed contrast is more prominent in summer than in winter, attributable to the elevated temperature variations.

Regional advantages in electricity sector investments, linked to atmospheric carbon concentration, are predominantly centered around renewables. This trend is evident in the analysis of twelve distinct scenarios tailored for all EU countries with a time horizon of 2050, ensuring that investment strategies align with the dynamic nature of climate-affected power supply and the thermal characteristics of critical system components. Furthermore, the use of $\mathrm{qDTR_H}$ data reveals a reduction in transmission planning costs, harnessing the flexibility of the generation system, with a particularly notable effect in the scenarios tailored for France.

The introduction of qDTR opens a new avenue for curtailing reductions. Our results demonstrate, across all CO_2 targets and emission scenarios, the pivotal role of qDTR in enabling greater utilization of renewables without the need for storage technology. As an illustration, in France, with the CO_2 and $\mathrm{qDTR_{RCP\ 2.6}}$ scenarios, curtailment sees a reduction of up to 59% compared to $\mathrm{STR_H}$. This reduction translates into enhanced network transmission capacity and a higher capacity expansion for renewable energy.

3 Conclusions

Overall, this work confirms that 1) predicted climate, with higher ambient temperatures, causes a reduction in power system transmission capacity, in the region of 1.53%, 2.3%, and 0.2% for OHL, PT, and UGL, respectively. 2) the qDTR approach proposed, allows for higher transmission capacities, overcoming the rating reduction caused by climate change, as it improves component capacity by up to 35% on average during winter for PT and up to 14% during nighttime hours for OHL. 3) Overall network costs change modestly and we achieve a consistent reduction in renewable production curtailment.

4 Method

4.1 Overview

We develop a procedure to quantify the impact of climate change on power grid transmission capacity. This method is described in Fig. 7 and can be divided into two steps:

1) Firstly, DTR and qDTR are estimated for OHL, PT, and UGC [29] using thermal models of the components and weather data from historical reanalysis and climatic projections. This allows us to quantify the variation in transmission capacity due to climate change. 2) Secondly, a G&TEP is calculated with a horizon of 2050, using transmission capacities calculated with historical weather reanalysis, RCP, STR, and qDTR. This allows us to quantify the impact of climate change on transmission capacity calculated in the previous step.

4.2 Data

The data used in this study can be divided into two broad categories: (c) component data (static) and (a) environment data (static and dynamic). Historical meteorological conditions in Europe for the period 1970-2020 are obtained from ERA reanalysis [2], whilst climatic projections for the period 2020-2070 are obtained from the Copernicus Climate Change Service (C3S)[1]. Additional (b) soil properties for underground cable rating calculations are obtained from [30, 31]. A list of the parameters used and their source is reported in Table. 3. Component parameters, relative to the most popular elements, are obtained from the existing literature or data sheets provided by the main manufacturers such as [32] for OHL, [33] for UGC, and [34] for PT.

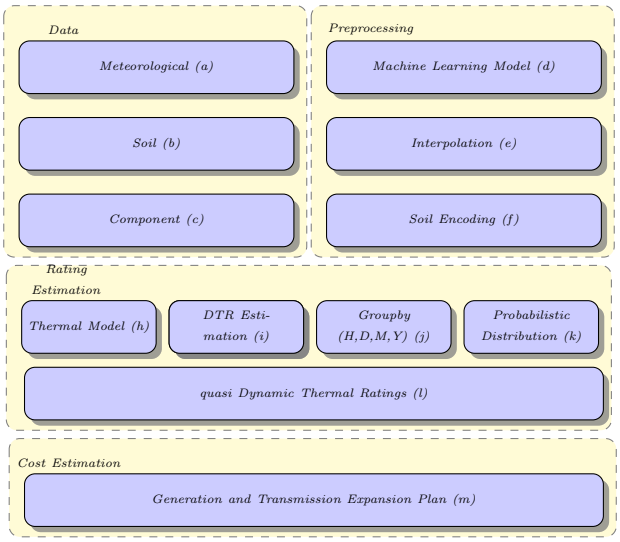

Figure 7: Visual representation of the procedure used in this study

Table 3: Summary of data and sources. a:ERA[1, 2], b:ISMN[30], c:ESDAC [31]. Soil composition: Silt, sand, clay, organic, bulk, texture

Parameter, Units	**Unit**	**Source**
Air temperature at 2 m	$^{\circ}C$ - θa	a
Total precipitation	$^{\text{mm}}$ - σ	a
Net surface solar radiation	$^{\text{Jm}^{-2}}$- H	a
u - v - wind at 10 m	$^{ms^{-1}}$- Ws	a
Soil composition	%	b, c
Soil Temperature	$^{\text{Jm}^{-2}}$- θs	b
Soil Moisture	$^{\text{Jm}^{-2}}$- ψs	b

4.3 Preprocessing

The raw data described are preprocessed as follows: (e) time series are uniformed by linear interpolation to a common time step of 1h. When a specific coordinate is required, parameters are interpolated linearly from the four nearest available grid points. (d, f) soil temperature and soil moisture are calculated using a dedicated machine-learning-based model for each coordinate. This is necessary since the available values from [1] are either not obtainable at the typical UGC burial depth (1-5m, in the case of soil temperature) or absent (in the case of soil moisture).

4.4 Rating estimation

The estimation of ratings starts with the use of (h) component thermal models based on the thermal balance between the heat generated by the Joule effect I^2R and the heat dissipated in the environment by convection or conductivity Q_c, radiation Q_r and the solar heat gain Q_s. This is shown in Eq. 1, where the parameters are influenced by: surface absorptivity for α, surface emissivity, maximum allowable temperature T_c and air temperature T_a for β. The parameter γ depends on atmospheric values such as wind speed W_s and T_a for OHL, and soil parameters such as soil temperature T_s and soil moisture ψ_s for UGC.

$$I^2R + \alpha Q_s = \beta Q_r + \gamma Q_c \tag{1}$$

The state of the art thermal models for OHL [35], UGC [36] and PTR [37] are used to compute the DTR (i) for each power component at each coordinate and each hourly time steps available in the datasets [1, 2].

At this point, (j) the simulated historical or future DTRs are grouped by time interval (yearly, monthly, monthly/hourly, etc.). For each group, a power law function is fitted to the lowest tail of the distribution (k). Finally, an accepted risk for thermal overload is chosen, $x = 0.1\%$ in this work, and the qDTR in terms of current intensity I are calculated (l) as in Eq. 2.

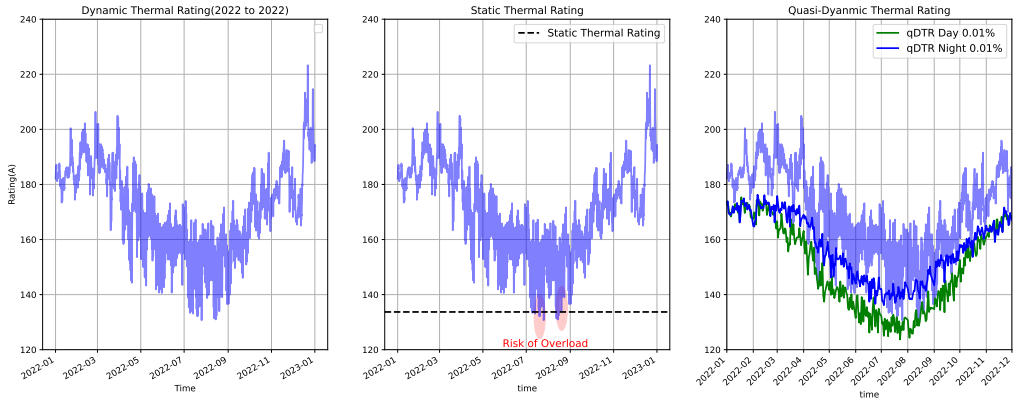

Figure 8: Conceptual illustrations of power system component rating capacities can be categorized into different methods. For DTR, a thermal model is utilized to compute the maximum capacity, taking into account real-time variables. Contrastingly, for STRs, a fixed value is applied throughout the year as a constrained capacity limit, without considering changing conditions. qDTR, calculates a 0.1% overload risk over the lower tail values of DTR across a 50-year time horizon. Notably, cooler forced temperatures and lower irradiation levels increase the capacity during the winter season and nighttime hours.

$$I(x) = Ax^{\alpha} \tag{2}$$

4.5 Costs estimation

The financial impacts resulting from the reduction in DTR due to climate change are assessed through a series of G&TEP using [38] and CO_2 budgets for the RCP from [39, 40, 41, 42, 43, 44, 45] . These studies rely on the use of yearly STRs, and monthly/hourly DTRs (mhDTR), equivalent to 288 DTRs calculated for each month/hour combination. Several comparisons are carried out:

1) G&TEP are carried out using $\mathrm{STR_H}$ calculated on a historical reanalysis and $\mathrm{qDTR_{RCP}}$ on the three climatic projections. The comparison shows the error incurred when not considering the impact of climate change on transmission capacity.

2) G&TEP are carried out using $\mathrm{STR_H}$ and monthly/hourly $\mathrm{qDTR_H}$ calculated from historical reanalysis. The comparison shows the benefits of using frequently changing qDTR to recover the lost transmission capacity.

References

[1] Copernicus Climate Change Service (2021): Climate and energy indicators for Europe from 2005 to 2100 derived from climate projections. Copernicus Climate Change Service (C3S) Climate Data Store (CDS), 2021. Accessed on 14-03-2023.

[2] Bell B. Hersbach, P. Berrisford, G. Biavati, A. Horányi, J. Muñoz Sabater, Nicolas, C. Peubey, R. Radu, I. Rozum, D. Schepers, A. Simmons, C. Soci, D. Dee, and Thépaut. ERA5 hourly data on single levels from 1940 to present, 2023. Accessed on 14-03-2023.

[3] Matthew. Bartos et al. Impacts of rising air temperatures on electric transmission ampacity and peak electricity load in the united states. *Environmental Research Letters*.

[4] Seleshi G Yalew, Michelle TH van Vliet, David EHJ Gernaat, Fulco Ludwig, Ariel Miara, Chan Park, Edward Byers, Enrica De Cian, Franziska Piontek, Gokul Iyer, et al. Impacts of climate change on energy systems in global and regional scenarios. *Nature Energy*, 5(10):794–802, 2020.

[5] Y. Romitti and I. Sue Wing. Heterogeneous climate change impacts on electricity demand in world cities circa mid-century. *Sci Rep*, 12:4280, 2022.

[6] Juan A. Añel, Manuel Fernández-González, Xavier Labandeira, Xiral López-Otero, and Laura De la Torre. Impact of cold waves and heat waves on the energy production sector. *Atmosphere*, 8(11), 2017.

[7] U.S. Department of Energy. Annual u.s. transmission data review. Technical report, 2018.

[8] Soheila Karimi, Petr Musilek, and Andrew M. Knight. Dynamic thermal rating of transmission lines: A review. *Renewable and Sustainable Energy Reviews*, 91:600–612, 2018.

[9] Behzad Keyvani, Eoin Whelan, Eadaoin Doddy, and Damian Flynn. Indirect weather-based approaches for increasing power transfer capabilities of electrical transmission networks. *WIREs Energy and Environment*, 12(3):e470, 2023.

[10] Dale A. Douglass, Jake Gentle, Huu-Minh Nguyen, William Chisholm, Charles Xu, Tip Goodwin, Hong Chen, Sarma Nuthalapati, Neil Hurst, Ian Grant, Jose Antonio Jardini, Robert Kluge, Paula Traynor, and Cody Davis. A review of dynamic thermal line rating methods with forecasting. *IEEE Transactions on Power Delivery*, 34(6):2100–2109, 2019.

[11] Soheila Karimi, Petr Musilek, and Andrew M. Knight. Dynamic thermal rating of transmission lines: A review. *Renewable and Sustainable Energy Reviews*, 91:600–612, 2018.

[12] Philipp Glaum and Fabian Hofmann. Enhancing the german transmission grid through dynamic line rating. In *2022 18th International Conference on the European Energy Market (EEM)*, pages 1–7, 2022.

[13] Andrej Trpovski and Thomas Hamacher. A comparative analysis of transmission system planning for overhead and underground power systems using ac and dc power flow. In *2019 IEEE PES Innovative Smart Grid Technologies Europe (ISGT-Europe)*, pages 1–5, 2019.

[14] SeyedeFatemeh Hajeforosh, Amena Khatun, and Math Bollen. Enhancing the hosting capacity of distribution transformers for using dynamic component rating. *International Journal of Electrical Power Energy Systems*, 142:108130, 2022.

[15] Oscar David Ariza Rocha, Kateryna Morozovska, Tor Laneryd, Ola Ivarsson, Claes Ahlrot, and Patrik Hilber. Dynamic rating assists cost-effective expansion of wind farms by utilizing the hidden capacity of transformers. *International Journal of Electrical Power Energy Systems*, 123:106188, 2020.

[16] Jiashen Teh and Ching-Ming Lai. Reliability impacts of the dynamic thermal rating and battery energy storage systems on wind-integrated power networks. *Sustainable Energy, Grids and Networks*, 20:100268, 2019.

[17] Ching-Ming Lai and Jiashen Teh. Network topology optimisation based on dynamic thermal rating and battery storage systems for improved wind penetration and reliability. *Applied Energy*, 305:117837, 2022.

[18] Kateryna Morozovska. *Dynamic rating with applications to renewable energy.* PhD thesis, KTH Royal Institute of Technology, 2020.

[19] Andrea Michiorri, Huu-Minh Nguyen, Stefano Alessandrini, John Bjørnar Bremnes, Silke Dierer, Enrico Ferrero, Bjørn-Egil Nygaard, Pierre Pinson, Nikolaos Thomaidis, and Sanna Uski. Forecasting for dynamic line rating. *Renewable and Sustainable Energy Reviews*, 52:1713–1730, 2015.

[20] Dale Douglass, William Chisholm, Glenn Davidson, Ian Grant, Keith Lindsey, Mark Lancaster, Dan Lawry, Tom McCarthy, Carlos Nascimento, Mohammad Pasha, Jerry Reding, Tapani Seppa, Janos Toth, and Peter Waltz. Real-time overhead transmission-line monitoring for dynamic rating. *IEEE Transactions on Power Delivery*, 31(3):921–927, 2016.

[21] Mohammad Mahmoudian Esfahani and Gholam Reza Yousefi. Real time congestion management in power systems considering quasi-dynamic thermal rating and congestion clearing time. *IEEE Transactions on Industrial Informatics*, 12(2):745–754, 2016.

[22] International Electrotechnical Commission (IEC). Iec 60076-7:2018, power transformers - part 7: Loading guide for mineral-oil-immersed power transformers. Technical report, International Electrotechnical Commission (IEC), 2018.

[23] International Electrotechnical Commission. Iec 60287-1-1: Electric cables—calculation of the current rating—part 1-1: Current rating equations (100% load factor) and calculation of losses—general. Technical report, International Electrotechnical Commission, Geneva, Switzerland, 2014.

[24] Javier Iglesias, George Watt, Dale Douglass, Vincent Morgan, Rob Stephen, Mark Bertinat, Dzevad Muftic, Ralph Puffer, Daniel Guery, Sidnei Ueda, Kesimir Bakic, Sven Hoffmann, Tapani Seppa, Franc Jakl, Carlos Do Nascimento, Francesco Zanellato, and Huu-Minh Nguyen. *Guide for Thermal Rating Calculations of Overhead Lines.* CIGRE Technical brochure N° 601. CIGRE, December 2014.

[25] Tom Brown, David Schlachtberger, Alexander Kies, Stefan Schramm, and Martin Greiner. PyPSA-Eur: An open optimisation model of the european electricity system. *Zenodo*, 2020.

[26] Karl Taylor, Ronald Stoufer, and Gerald Meehl. An overview of cmip5 and the experiment design. *Bull. Am. Meteorol. Soc.*, 93:485–498, 2011.

[27] Keywan Riahi, Detlef P. van Vuuren, Elmar Kriegler, Jae Edmonds, Brian C. O'Neill, Shinichiro Fujimori, Nico Bauer, Katherine Calvin, Rob Dellink, Oliver Fricko, Wolfgang Lutz, Alexander Popp, Jesus Crespo Cuaresma, Samir KC, Marian Leimbach, Leiwen Jiang, Tom Kram, Shilpa Rao, Johannes Emmerling, Kristie Ebi, Tomoko Hasegawa, Petr Havlik, Florian Humpenöder, Lara Aleluia Da Silva, Steve Smith, Elke Stehfest, Valentina Bosetti, Jiyong Eom, David Gernaat, Toshihiko Masui, Joeri Rogelj, Jessica Strefler, Laurent Drouet, Volker Krey, Gunnar Luderer, Mathijs Harmsen, Kiyoshi

Takahashi, Lavinia Baumstark, Jonathan C. Doelman, Mikiko Kainuma, Zbigniew Klimont, Giacomo Marangoni, Hermann Lotze-Campen, Michael Obersteiner, Andrzej Tabeau, and Massimo Tavoni. The shared socioeconomic pathways and their energy, land use, and greenhouse gas emissions implications: An overview. *Global Environmental Change*, 42:153–168, 2017.

[28] Carsten Matke, Wided Medjroubi, and David Kleinhans. SciGRID - An Open Source Reference Model for the European Transmission Network (v0.2), July 2016.

[29] Sergio Montana and Michiorri Andrea. Long-term dynamic thermal ratings of underground cables integrating soil dynamics and climate projections. https://hal.science/hal-04453943.

[30] W. Dorigo and et al Himmelbauer. The international soil moisture network: serving earth system science for over a decade. *Hydrology and Earth System Sciences*, 25(11):5749–5804, 2021.

[31] Roland Hiederer. *Mapping Soil Properties for Europe - Spatial Representation of Soil Database Attributes*. EUR26082EN Scientific and Technical Research. Publications Office of the European Union, Luxembourg, 2013.

[32] E. Kiessling, P. Nefzger, J.E. Nolasco, and U. Kaintzyk. *Overhead Power Lines Planning, Design, Construction – Hard-drawn AL1 ACSR*. PublisherName, City, edition edition, 2019.

[33] TELE-FONIKA Kable S.A. *High and extra high voltage cables*. www.tfkable.com, City, edition edition, 2019. https://www.tfkable.com/en$_p l/catalogs - and - brochures/catalogues.html$.

[34] 529 Working Group A2.36. Guidelines for conducting design reviews for power transformers. Technical Report Report Number, Publisher Name, April 2013.

[35] Javier Iglesias, George Watt, Dale Douglass, Vincent Morgan, Rob Stephen, Mark Bertinat, Dzevad Muftic, Ralf Puffer, Daniel Guery, Sidnei Ueda, Kresimir Bakic, and Sven Hoffmann. Guide for thermal rating calculations of overhead lines. Research Paper CIGRE 601, CIGRE, Paris, 2014.

[36] Electric cables – calculation of the current rating – part 1-1: Current rating equations (100% load factor) and calculation of losses – general, 2014.

[37] Iec 60076-7:2018 - power transformers - part 7: Loading guide for mineral-oil-immersed power transformers. 2018.

[38] T. Brown, J. Hörsch, and D. Schlachtberger. PyPSA: Python for Power System Analysis. *Journal of Open Research Software*, 6(4), 2018.

[39] D. van Vuuren, M. den Elzen, P. Lucas, B. Eickhout, B. Strengers, B. van Ruijven, S. Wonink, and R. van Houdt. Stabilizing greenhouse gas concentrations at low levels: an assessment of reduction strategies and costs. *Climatic Change*, 2007.

[40] L. Clarke, J. Edmonds, H. Jacoby, H. Pitcher, J. Reilly, and R. Richels. Scenarios of greenhouse gas emissions and atmospheric concentrations. Sub-report 2.1a of synthesis and assessment product 2.1, U.S. Climate Change Science Program and the Subcommittee on Global Change Research, Department of Energy, Office of Biological & Environmental Research, Washington, DC, USA, 2007.

[41] S.J. Smith and T.M.L. Wigley. Multi-gas forcing stabilization with the minicam. *Energy Journal (Special Issue 3)*, pages 373–391, 2006.

[42] M.A. Wise, K.V. Calvin, A.M. Thomson, L.E. Clarke, B. Bond-Lamberty, R.D. Sands, S.J. Smith, A.C. Janetos, and J.A. Edmonds. Implications of limiting co2 concentrations for land use and energy. *Science*, 324:1183–1186, May 29 2009.

[43] J. Fujino, R. Nair, M. Kainuma, T. Masui, and Y. Matsuoka. Multi-gas mitigation analysis on stabilization scenarios using aim global model. *Multigas Mitigation and Climate Policy. The Energy Journal Special Issue*, 2006.

[44] Y. Hijioka, Y. Matsuoka, H. Nishimoto, M. Masui, and M. Kainuma. Global ghg emissions scenarios under ghg concentration stabilization targets. *Journal of Global Environmental Engineering*, 13:97–108, 2008.

[45] K. Riahi, A. Gruebler, and N. Nakicenovic. Scenarios of long-term socio-economic and environmental development under climate stabilization. *Technological Forecasting and Social Change*, 74(7):887–935, 2007.

5 Annex

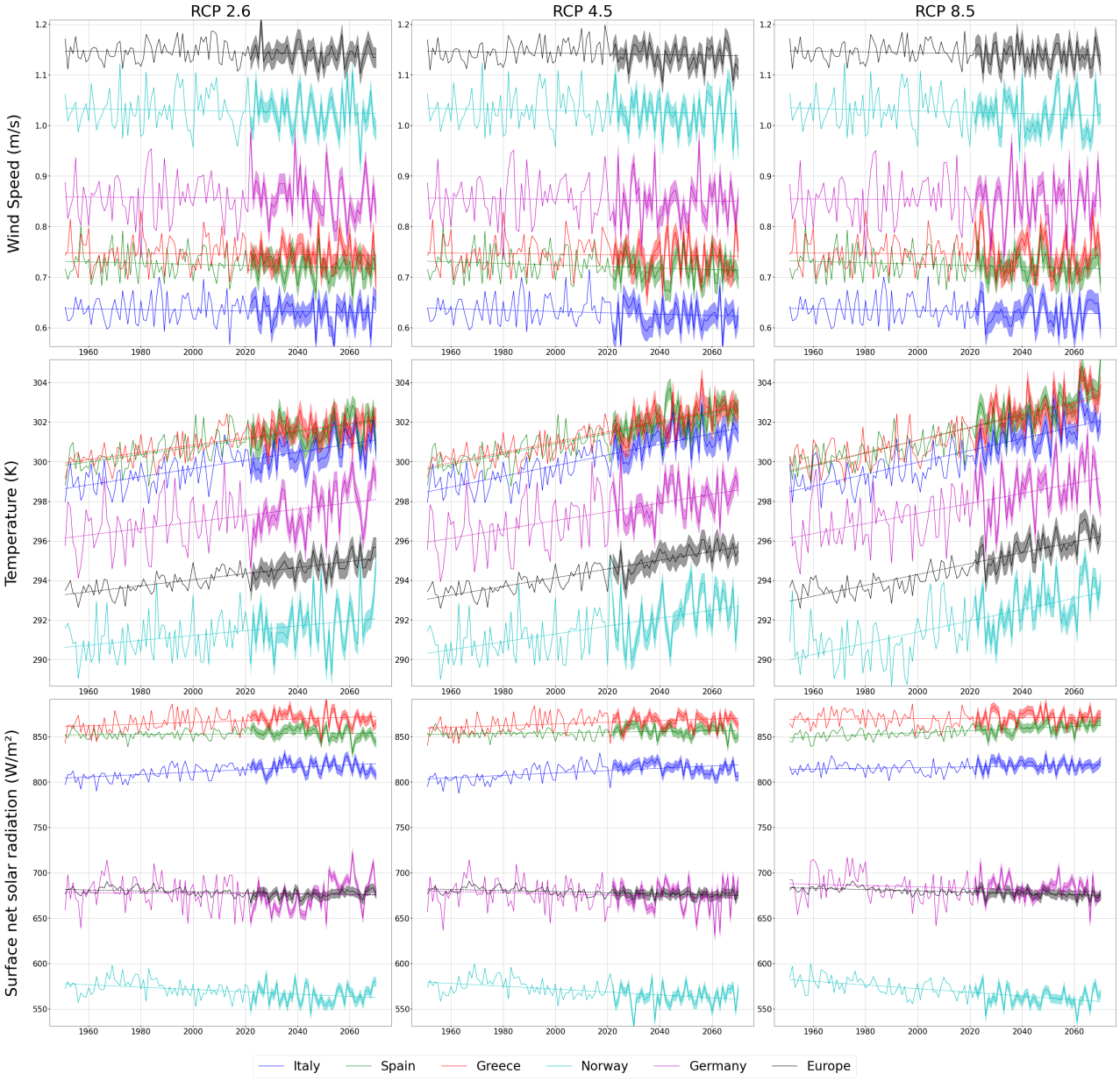

Figure 9: Meteorological change projection , evaluated rolling mean for 2.6, 4.5, 8.5 RCP and the 2nd percentile values for each region